Exploring massive neutrinos in dark cosmologies with EFTCAMB/EFTCosmoMC

Bin Hu,[1] Marco Raveri,[2,3] Alessandra Silvestri,[1] and Noemi Frusciante[2,3]

[1]*Institute Lorentz, Leiden University, PO Box 9506, Leiden 2300 RA, The Netherlands*
[2]*SISSA - International School for Advanced Studies, Via Bonomea 265, 34136, Trieste, Italy*
[3]*INFN, Sezione di Trieste, Via Valerio 2, I-34127 Trieste, Italy*

We revisit the degeneracy between massive neutrinos and generalized theories of gravity in the framework of the effective field theory of cosmic acceleration. In particular, we consider $f(R)$ theories and a class of nonminimally coupled models parametrized via a coupling to gravity which is linear in the scale factor. In the former case, we find a slightly lower degeneracy with that found in the literature, due to the fact that we implement exact designer $f(R)$ models and evolve the full linear dynamics of perturbations. As a consequence, our bounds are slightly tighter on the $f(R)$ parameter but looser on the summed neutrino mass. We also set a new upper bound on the Compton wavelength parameter $\mathrm{Log}_{10}B_0 < -4.1$ at 95% C.L. with a fixed summed neutrino mass ($\sum m_\nu = 0.06$ eV) in $f(R)$ gravity with the combined data sets from cosmic microwave background temperature and lensing power spectra of the Planck Collaboration, as well as galaxy power spectrum from the WiggleZ dark energy survey. We do not observe a sizable degeneracy between massive neutrinos and modified gravity in the nonminimally coupled model considered, which corresponds to a peculiar case of coupling that depends linearly on the scale factor. The analysis is performed with an updated version of the EFTCAMB/EFTCosmoMC package, which is now publicly available and extends the first version of the code with the consistent inclusion of massive neutrinos, tensor modes, several alternative background histories, and designer quintessence models.

I. INTRODUCTION

The direct measurements of neutrino flavor oscillations provide evidence for nonzero neutrino masses, but give no hint as to their absolute mass scale (see, e.g., the reviews [1,2]). Cosmology, on the other hand, provides a powerful, complementary way of placing constraints on the sum of the mass of neutrinos (see, e.g., the reviews [3,4]). Indeed, massive neutrinos can significantly affect the distribution of large-scale structure (LSS) and the pattern of cosmic microwave background (CMB) anisotropies depending on the value of their mass. The current constraint from CMB experiments on the summed neutrino mass fixes the upper limit at $\sum m_\nu < 0.66$ eV (95%; Planck + WP+ highL) for a flat Λ cold dark matter (ΛCDM) cosmology [5]. Besides slightly affecting the expansion history, massive neutrinos leave an imprint on the dynamics of linear scalar perturbations. On scales smaller than their mass scale neutrinos free stream, damping the structure and accordingly diminishing the weak lensing effect on those scales [6]. Furthermore, they contribute an early integrated Sachs-Wolfe (ISW) effect because their transition from relativistic to nonrelativistic happens on an extended redshift interval which, for the typical neutrino mass ($\sum m_\nu \sim 0.1$ eV), overlaps with the transition from radiation to matter [6].

Similar effects are also observed in dark energy (DE) and modified gravity (MG) models that address the phenomenon of cosmic acceleration. The latter generally involves an extra, dynamical massive scalar degree of freedom (d.o.f.) which mediates a fifth force between matter particles and can have a speed of sound different from unity. Besides affecting the background dynamics (such as driving the late-time cosmic acceleration), on linear scales the field can significantly modify the clustering of matter as well as the subhorizon dynamics of metric potentials on scales below or above its characteristic length scale. Hence, structure formation, the ISW effect, and the weak lensing effect will be modified accordingly [7–9]. Based on these considerations, a degeneracy between massive neutrinos and the dark sector is expected, and in general neutrino bounds depend significantly on the cosmological model within which they are analyzed. This has been investigated by several authors [10–14].

In this paper we investigate the degeneracy between massive neutrinos and cosmological models which deviate from general relativity by the inclusion of an extra scalar d.o.f. in the framework of effective field theory (EFT). In particular, we extensively analyze $f(R)$ theories, with the designer approach, updating the bound on the Compton scale parameter B_0 with and without a massive neutrino. We also consider a linear EFT parametrization of nonminimally coupled models. We use mainly CMB and LSS observables, as described in detail in Sec. II. The present investigation is made by means of EFTCAMB and EFTCosmoMC [15,16]. These are patches of CAMB/CosmoMC [17–19] which allow one to investigate the

evolution of linear perturbations in a model-independent way, as well as in any specific DE/MG model that can be cast into an EFT framework of cosmic acceleration formulated by Refs. [20–22].

A new release of EFTCAMB which is fully compatible with massive neutrinos is now available at http://wwwhome.lorentz.leidenuniv.nl/~hu/codes/. Let us note that the new version of EFTCAMB/EFTCosmoMC has also been equipped with several alternative DE equation-of-state parametrizations [23–25], the tensor perturbation equation, and designer minimally coupled quintessence models. This release comes with detailed notes [26].

II. OBSERVABLES AND DATA

In our analysis we will use different combinations of the following data sets. We employ the Planck temperature-temperature (TT) power spectra considering the nine frequency channels ranging from 30–353 GHz for low-ℓ modes ($2 \leq \ell < 50$) and the 100, 143, and 217 GHz frequency channels for high-ℓ modes ($50 \leq \ell \leq 2500$) [5,27]. In addition, we include the WMAP low-ℓ polarization spectra ($2 \leq \ell \leq 32$) [28] in order to break the degeneracy between the reionization optical depth and the amplitude of CMB temperature anisotropy. In the following we will denote the combination of the two above data sets as Planck Likelihood Code (PLC). We also include the Planck 2013 full-sky lensing potential map [29], obtained by using the 100, 143, and 217 GHz frequency bands that resulted in a detection of the CMB lensing signal with a significance greater than 25σ. We will refer to this data set as the lensing one. The baryon acoustic oscillations (BAO) measurements are taken from the 6dFGS ($z = 0.1$) [30], SDSS DR7 (at effective redshift $z_{\rm eff} = 0.35$) [31,32], and BOSS DR9 ($z_{\rm eff} = 0.2$ and $z_{\rm eff} = 0.35$) [33] surveys. Finally, we use measurements of the galaxy power spectrum as made by the WiggleZ Dark Energy Survey [34] in order to exploit the constraining power of data from large-scale structure. This latter data set consists of the galaxy power spectrum measured from spectroscopic redshifts of 170 352 blue emission-line galaxies over a volume of 1 Gpc^3 [35,36], and the covariance matrices as given in Ref. [36] are computed using the method described in Ref. [37]. It has been shown that linear theory predictions are a good fit to the data regardless of nonlinear corrections up to a scale of $k \sim 0.2$ h/Mpc [12,36], and for this reason we use the WiggleZ galaxy power spectrum with $k_{\rm max} = 0.2$ h/Mpc. Finally, we marginalize over a linear galaxy bias for each of the four redshift bins, as in Ref. [36].

III. A WORKED EXAMPLE I: MASSIVE NEUTRINOS AND $f(R)$ MODELS

As we discussed in the Introduction, massive neutrinos are an extension of the cosmological standard model which modify the dynamics of linear scalar perturbations, leaving

a characteristic imprint on the growth of structure [3]. Specifically, on linear scales smaller than the neutrino free-streaming distance, the overall matter clustering is suppressed. Interestingly, scalar-tensor models of modified gravity leave a complementary signature on the growth of structure, enhancing the clustering on linear scales within the Compton scale of the extra scalar degree of freedom, because of the fifth force mediated by the latter. Depending on the mass of the neutrinos and of the scalar field, there may be a significant degeneracy between the two effects at some redshifts and scales. The latter has been investigated to a large extent in the context of $f(R)$ theories of gravity, and generally an appreciable degeneracy has been found. However, a common feature of all previous analyses is the assumption of the quasistatic (QS) limit in the equations for the perturbations and the employment of the QS parametrization introduced by Bertschinger and Zukin in Ref. [38]. In this paper we revisit this degeneracy using EFTCAMB, which has the important virtue of letting us implement exact $f(R)$ models and evolve their full dynamics. Another key feature of our analyses is the consistent treatment of the background cosmology, which is based on a designer reconstruction of $f(R)$ models with the inclusion of massive neutrinos.

A. Numerical implementation of $f(R)$ models

We shall now discuss in some detail the implementation of $f(R)$ models in EFTCAMB. We will then review their implementation in MGCAMB [13,39], since in the following subsection we will compare the results obtained with these two codes.

$f(R)$ gravity is described by the following action in the Jordan frame:

$$S = \frac{M_P^2}{2} \int d^4x \sqrt{-g}[R + f(R)] + S_m, \qquad (1)$$

where $f(R)$ is a general function of the Ricci scalar R, and S_m is the matter action whose Lagrangian is minimally coupled to gravity. For a detailed review of the cosmology of $f(R)$ theories we refer the reader to Refs. [40–42]. Despite the fourth-order nature of the $f(R)$ field equations, it can be shown that the above action belongs to the class of scalar-tensor theories with second-order field equations, where the role of the scalar d.o.f. is played by $f_R \equiv df/dR$, commonly dubbed the scalaron [43]. The dynamics of linear scalar perturbations in models of $f(R)$ gravity has been extensively studied in Refs. [44–46]. Here, we shall focus on the designer approach to $f(R)$ theories that EFTCAMB exploits. It was introduced in Ref. [44] and offers a practical way of reconstructing all $f(R)$ models that reproduce a given expansion history. Once the latter is chosen, the modified Friedmann equation can be solved as a second-order differential equation for $f[R(a)]$. While the original setup only considered dust in the energy budget of

the Universe, in Ref. [46] the approach was extended to include radiation and in Ref. [11] to also include massive neutrinos via the approximation adopted by WMAP7 [47]. Here, we consistently include the massless/massive neutrino sector in the designer formalism by using instead the formula adopted by CAMB [6,48].

Let us define the following dimensionless quantities:

$$y \equiv \frac{f(R)}{H_0^2}, \qquad E \equiv \frac{H^2}{H_0^2} = E_m + E_r + E_\nu + E_{\rm eff}, \quad (2)$$

with

$$E_m = \Omega_m a^{-3}, \qquad E_r = \Omega_r a^{-4}, \qquad E_\nu = \frac{8\pi G}{3H_0^2}\rho_\nu,$$

$$E_{\rm eff} = \Omega_{\rm eff} \exp\left[-3\ln a + 3\int_a^1 w_{\rm eff}(\tilde{a})d\ln\tilde{a}\right], \quad (3)$$

where the gravity modifications are treated as an effective dark fluid with an equation of state $w_{\rm eff}(a)$, and where we have enforced flatness, $\Omega_{\rm eff} = 1 - \Omega_m - \Omega_r - \Omega_\nu$. To be clear, here the subscripts "m," "r," and "ν" denote, respectively, nonrelativistic matter (baryons and CDM), photons, and neutrinos (including both massless and massive species). We assume that all massive neutrino species have equal masses and that neutrino decoupling in the early Universe is instantaneous [6], so that their distribution function is given by the Fermi-Dirac distribution.

When neutrinos are in the relativistic regime their momentum is large compared to their rest mass, $q \gg m_\nu a$, and their energy density and pressure are given by

$$\rho_\nu = \rho_{\nu(m=0)}\left(1 + \frac{5}{7\pi^2}\bar{m}^2 a^2\right),$$

$$P_\nu = \frac{1}{3}\rho_{\nu(m=0)}\left(1 - \frac{5}{7\pi^2}\bar{m}^2 a^2\right), \quad (4)$$

where $\rho_{\nu(m=0)} = N_{\rm eff} 7/8(4/11)^{4/3}\rho_r$ and $\bar{m} = m_\nu/k_B T_d a_d$ are the massless neutrino density and dimensionless neutrino mass parameter, respectively. $N_{\rm eff}$ is the effective number of neutrino species whose standard value is 3.046 [49,50], and T_d and a_d are the temperature and scale factor at neutrino decoupling, respectively. In the nonrelativistic regime the bulk of the neutrinos have $q \ll m_\nu a$ and their energy density and pressure evolve in the Friedman-Robertson-Walker limit as

$$\rho_\nu \simeq \frac{180}{7\pi^4}\rho_{\nu(m=0)}\left(\zeta_3\bar{m}a + \frac{15\zeta_5}{2\bar{m}a} - \frac{945\zeta_7}{16(\bar{m}a)^3} + \cdots\right),$$

$$P_\nu \simeq \frac{900}{7\pi^4}\rho_{\nu(m=0)}\left(\frac{\zeta_5}{\bar{m}a} - \frac{63}{4}\frac{\zeta_7}{(\bar{m}a)^3} + \cdots\right), \quad (5)$$

where ζ_s are Riemann zeta functions. In the intermediate regime their density and pressure are given by the numerical integral of the Fermi-Dirac distribution.

As shown in Ref. [44], the Friedmann equation for $f(R)$ theories can be written as a second-order differential equation for y,

$$y'' - \left(1 + \frac{E'}{2E} + \frac{R''}{R'}\right)y' + \frac{R'}{6H_0^2 E}y = -\frac{R'}{H_0^2 E}E_{\rm eff}, \quad (6)$$

where a prime indicates derivation with respect to $\ln a$ and H_0 is the present-day Hubble parameter. As written explicitly in Eq. (2), E also contains the contribution from neutrinos. We fix the initial conditions deep in the radiation-dominated epoch ($a \sim 10^{-8}$), when the effective dark component does not affect the evolution and the neutrinos are ultrarelativistic. The analysis in Ref. [46] is still valid, but the inclusion of massive neutrinos affects the physical processes after matter-radiation equality. In particular, their inclusion shifts the time of matter-radiation equality since at such early times neutrinos are in the ultrarelativistic regime. We emphasize that, in addition to the fitting formula of the neutrino sector, our work and Ref. [11] also differ in the epoch when the initial conditions of the designer approach are set up; in Ref. [11] the initial conditions were fixed in the matter-dominated era, while here they are set up during the radiation-dominated epoch.

After fixing the expansion history, we are ready to solve the designer equation (6). Following the argument in Ref. [44], we set the amplitude of the decaying mode to zero at the initial time, and we are left with only one free boundary condition. In other words, for a given expansion history we will find a family of $f(R)$ models reproducing it and differing by the boundary condition. The latter is typically chosen to coincide with the present day value, B_0, of the Compton wavelength in Hubble units,

$$B = \frac{2}{3(1+f_R)}\frac{1}{4E'+E''}\frac{E}{E'}\left(y'' - y'\frac{4E''+E'''}{4E'+E''}\right). \quad (7)$$

After an expansion history and a value for B_0 are chosen, EFTCAMB evolves the *full*, linear dynamics of perturbations for the corresponding $f(R)$ model. Things are different in the case when MGCAMB is used. While the framework at the basis of this code is in general not restricted to the quasistatic limit, the implementation of specific models like $f(R)$ relies on the parametrization introduced by Bertschinger and Zukin in Ref. [38], and later extended in Refs. [46,51,52], which is quasistatic and introduces an approximation for the time evolution of f_R. More specifically, the background is fixed to the desired one, which in this case is ΛCDM plus the parameter f_ν that models massive neutrinos. The effects of modified gravity are then taken into account via the following parametrization of Poisson and anisotropy equations:

$$k^2\Psi = -\mu(a,k)\frac{a^2}{2M_P^2}[\rho_m\Delta_m + 3(\rho_m + P_m)\sigma_m],$$

$$k^2[\Phi - \gamma(a,k)\Psi] = \mu(a,k)\frac{3a^2}{aM_P^2}(\rho_m + P_m)\sigma_m, \qquad (8)$$

where no QS limit has been taken, and σ_m is the anisotropic stress from matter, to which neutrinos are expected to contribute at high redshift.

If one wants to implement a specific model [in this case $f(R)$], one needs to reduce to the QS limit, so that the Einstein equations become a set of algebraic equations and it is easy to find an analytical expression for μ and γ. In the case of $f(R)$, they assume the following form [46]:

$$\mu = \frac{1}{1+f_R}\frac{1 + 4\frac{f_{RR}}{1+f_R}\frac{k^2}{a^2}}{1 + 3\frac{f_{RR}}{1+f_R}\frac{k^2}{a^2}}, \qquad \gamma = \frac{1 + 2\frac{f_{RR}}{1+f_R}\frac{k^2}{a^2}}{1 + 4\frac{f_{RR}}{1+f_R}\frac{k^2}{a^2}}. \qquad (9)$$

In the current setup of MGCAMB a further simplification is applied when treating $f(R)$ models, which reduces μ and γ to the following expressions in terms of a single parameter, B_0:

$$\mu = \frac{1}{1 - B_0\Omega_m a^3/2}\frac{1 + (2/3)B_0(k/H_0)^2 a^4}{1 + (1/2)B_0(k/H_0)^2 a^4},$$

$$\gamma = \frac{1 + (1/3)B_0(k/H_0)^2 a^4}{1 + (2/3)B_0(k/H_0)^2 a^4}, \qquad (10)$$

which correspond to a QS approximation with a power law to describe the time evolution of the Compton wavelength of the scalar d.o.f. [53]. Hereafter we will refer to Eq. (10) as the Bertschinger-Zukin (BZ) parametrization. Equation (10) is combined with the system of Boltzmann equations for matter components, and the dynamics of the linear scalar perturbations is evolved. They were numerically implemented in Refs. [13,39].

B. Results and discussion

Armed with the full and consistent treatment of the background cosmology for $f(R)$ theories in the presence of massive neutrinos, we can now turn our attention to the dynamics of linear scalar perturbations. While EFTCAMB provides a number of different parametrizations for the effective dark energy equation of state that can be used in conjunction with the $f(R)$ designer approach, in this paper we will consider only the case of a ΛCDM background. We compare our results with those obtained with the publicly available code MGCAMB [13,39], and in particular with the adapted version from Ref. [12]. We will focus on the constraints on the mass of the neutrinos and on the B_0 parameter labeling $f(R)$ theories.

Combining the different cosmological observables described in Sec. II, we explore constraints on designer $f(R)$ models in the massive neutrinos scenario, in the cases with either variable or fixed neutrino masses. The results are summarized in Table I. From there we can see that the PLC data set combined with BAO weakly constrain $f(R)$ models, so that in the range of interest there is no statistically significant upper bound on $\mathrm{Log}_{10}B_0$ in cases with either variable or fixed neutrino masses, even though the mass of the neutrinos is strongly constrained. This is because the constraining power of the CMB temperature-temperature spectrum on $f(R)$ models is dominated by the ISW effect on large scales. As shown in Refs. [54,55], the tension between the observed low value of large-scale multipoles of the CMB temperature-temperature spectrum and the ΛCDM prediction could indeed be reconciled by a large value for B_0 because of the ISW effect. On the other hand, the summed neutrino mass is better constrained by small-scale data and is affected negligibly by the tension in the low-ℓ multipoles. This is confirmed by the black line in Figs. 1(a) and 1(b), which clearly shows that the posterior probability distribution of $\mathrm{Log}_{10}B_0$ is peaked at a very large value because of this effect and regardless of the mass of the neutrinos. In the case of variable neutrino mass this pronounced peak results in a 2σ lower bound on $\mathrm{Log}_{10}B_0$, as can be seen from Table I. This comes from the fact that

TABLE I. Second column: Joint constraints on the B_0 parameter of designer $f(R)$ models and a variable neutrino mass. Third column: Constraints on B_0 in the case of a fixed neutrino mass ($\sum m_\nu = 0.06$ eV). In both cases, we use different combinations of the data sets described in Sec. II and the EFTCAMB code. The last three rows report the comparison between EFTCAMB, MGCAMB, and a quasistatic designer $f(R)$ code. These results are reported for the specific combinations of data used in Ref. [12] considering cases with either variable or fixed neutrino masses.

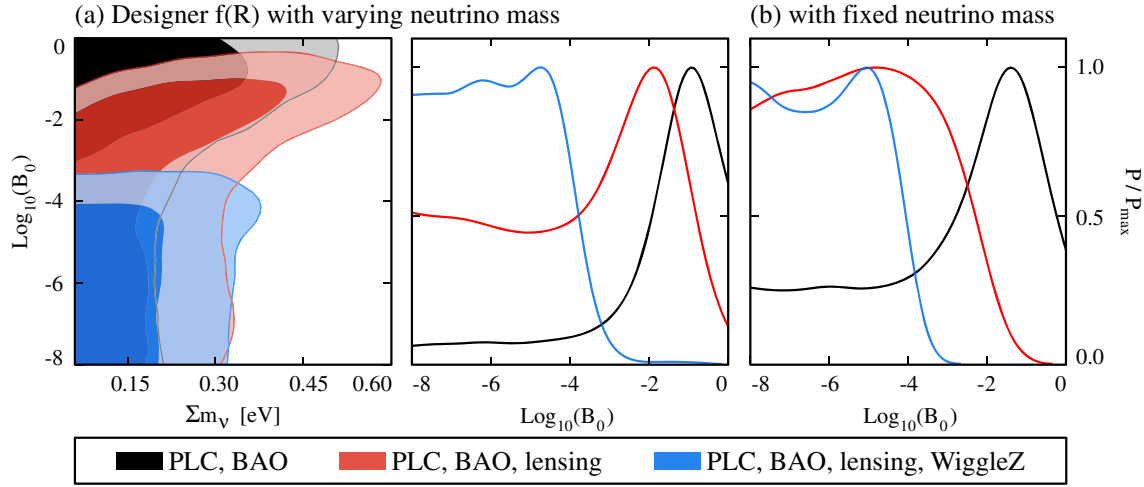| Data sets	Variable m_ν		Fixed m_ν
	$\mathrm{Log}_{10}B_0$ (95% C.L.)	$\sum m_\nu$ (95% C.L.)	$\mathrm{Log}_{10}B_0$ (95% C.L.)
PLC + BAO	> -6.35	< 0.37	none
PLC + BAO + lensing	< -1.0	< 0.43	< -2.3
PLC + BAO + lensing + WiggleZ	< -3.8	< 0.32	< -4.1
PLC + BAO + WiggleZ (EFTCAMB)	< -3.8	< 0.30	< -3.9
PLC + BAO + WiggleZ (QS $f(R)$)	< -3.2	< 0.24	< -3.7
PLC + BAO + WiggleZ (MGCAMB)	< -3.1	< 0.23	< -3.5

FIG. 1 (color online).   Left: The marginalized joint likelihood for the present day value of $\mathrm{Log}_{10}B_0$ and the sum of the neutrino masses, $\sum m_\nu$. Center and Right: The marginalized likelihood of $\mathrm{Log}_{10}B_0$ for, respectively, designer $f(R)$ models with variable (a) or fixed (b) neutrino masses. In all three panels different colors correspond to different combinations of cosmological observations, as shown in the legend. The darker and lighter shades correspond, respectively, to the 68% C.L. and 95% C.L.

models with large B_0 values are better fits for both the power deficit of the TT spectrum in the ISW regime and the relatively stronger lensing modulation of the TT spectrum around the third and fourth peaks, as found by Planck 2013. However, the inclusion of large-scale structure data disfavors large values of B_0 and the peak of the posterior distribution located at a nonzero value of B_0 loses its statistical significance after including other data sets, as we will discuss later. Moreover, as can be seen from Fig. 1, the PLC and BAO data compilation does not provide very robust constraints on the neutrino mass and Compton wavelength simultaneously (due to the degeneracy between these parameters), so that when the summed neutrino mass is fixed to the vanilla-model value, 0.06 eV, the tail of the distribution of $\mathrm{Log}_{10}B_0$ rises, resulting in no statistically significant lower bound on $\mathrm{Log}_{10}B_0$.

The whole picture slightly changes when CMB lensing data are added, since both $f(R)$ and massive neutrinos can affect these data significantly and in a degenerate way. As we already discussed, $f(R)$ models predict an enhancement of the growth on scales smaller than the Compton scale of the scalaron. Bigger values of B_0 correspond to larger Compton scales and hence a more significant enhancement of growth on linear scales. On the other hand, massive neutrinos predict a suppression of growth via free streaming and a shift in the matter-radiation equality time. Therefore, there is a degeneracy between B_0 and $\sum m_\nu$ when growth data are considered, with a nonzero neutrino mass allowing for larger values of B_0. This degeneracy is also reflected in the lensing effect imprinted by LSS on the CMB. Indeed, when lensing data are considered B_0 and $\sum m_\nu$ display a significant degeneracy, which is noticeable in Fig. 1(a). As can be seen from Table I, the marginalized bounds on the parameter of interest reflect this degeneracy. On the one hand, when lensing data are added the

constraint on the neutrino mass gets worse with respect to the CMB and BAO case; on the other hand, the constraint on $\mathrm{Log}_{10}B_0$ improves with respect to the CMB and BAO data-set combination, but it is worse with respect to the case in which lensing is included but the sum of the neutrino masses is not allowed to vary.

Comparing the one-dimensional likelihoods for B_0 (i.e., the red curves) in Figs. 1(b) and 1(c), we can see a significant difference in the bounds between the cases with variable and fixed neutrino masses. The present value of the Compton scale is well constrained when the neutrino mass is kept fixed ($\sum m_\nu = 0.06$ eV), with a bound of $\mathrm{Log}_{10}B_0 < -2.3$ at 95% C.L. Instead, when the neutrino mass is varied the bound is looser. In both cases the addition of CMB lensing data lifts the tail of the $\mathrm{Log}_{10}B_0$ distribution, removing any statistical significance from the lower bound found in the PLC and BAO case.

Finally, we can see that the addition of the WiggleZ data improves the situation. It is true that $f(R)$ and massive neutrinos leave a degenerate imprint on LSS; however, the constraining power of WiggleZ and its high sensitivity to changes in B_0 within the range that we consider are able to partially alleviate the degeneracy. Hence we obtain a stringent bound on B_0 when the mass of the neutrinos is fixed and, more generally, substantial bounds on both B_0 and $\sum m_\nu$ when the mass of the neutrinos is varied.

We compare our results with those obtained with MGCAMB, following the implementation described in Sec. III A. The results are in good agreement even though there are some interesting differences, which we shall discuss below. Form Table I we can see that the constraints obtained with EFTCAMB on $\mathrm{Log}_{10}B_0$ are a bit tighter, while the bound on the neutrino mass is weaker. The reason for this can be easily understood by looking at the marginalized joint likelihood of $\mathrm{Log}_{10}B_0$ and $\sum m_\nu$ in Fig. 2. From there
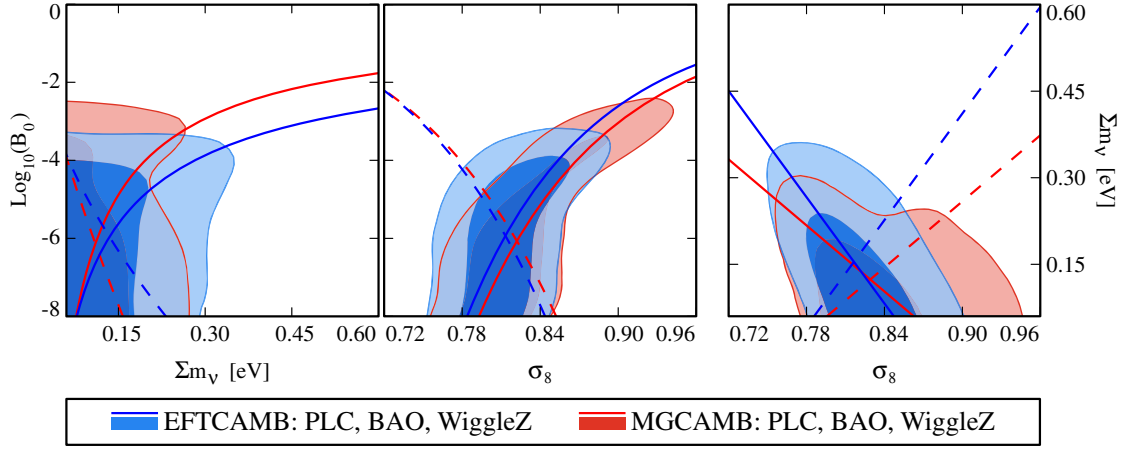
FIG. 2 (color online).   The marginalized joint likelihood for the present-day value of $Log_{10}B_0$, the sum of the neutrino masses, $\sum m_\nu$, and the amplitude of the (linear) power spectrum on the scale of $8h^{-1}$ Mpc, σ_8. Different colors correspond to the different codes used and, hence, a different modeling of $f(R)$, as shown in the legend. The darker and lighter shades correspond, respectively, to the 68% C.L. and 95% C.L. The solid line indicates the best-constrained direction in parameter space, while the dashed line indicates the least-constrained one. As we can see, these directions differ noticeably for the two codes.

we can see that there is a change in the degeneracy between these two parameters. This conclusion is further confirmed by looking at the principal components of the two parameters. These are shown in Fig. 2 as two lines: the continuous one corresponds to the best-constrained direction in parameter space, while the dashed one corresponds to the least-constrained one. The blue lines correspond to results obtained with EFTCAMB, while the red lines correspond to those obtained with MGCAMB. As we can see, the principal directions for the two codes differ noticeably. The same conclusion can be drawn from the other two panels of Fig. 2, where we can see that the degeneracies

between $Log_{10}B_0$, σ_8 and $\sum m_\nu$ change substantially. In particular, there is less degeneracy between σ_8 and $\sum m_\nu$ in $f(R)$ cosmologies when the analysis is performed with EFTCAMB.

These changes in the degeneracies are due to the different modeling of modified gravity physics. As discussed in Sec. III A, with respect to the complete $f(R)$ modeling of EFTCAMB the modeling of MGCAMB relies on two different assumptions, namely, the QS regime for the perturbation and the power-law ansatz for the time dependence of the Compton wavelength of the scalaron, which is characteristic of the BZ parametrization (10). In order to
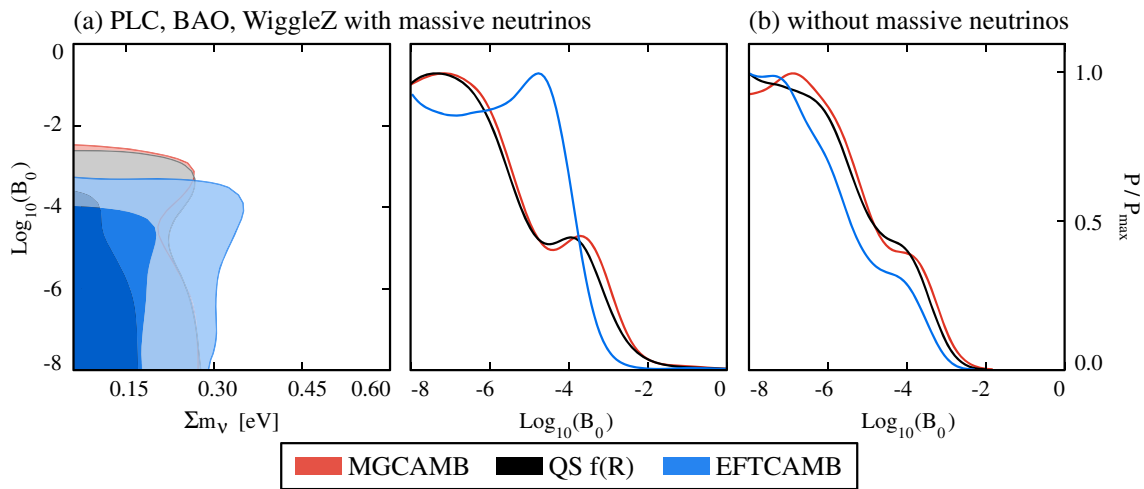

FIG. 3 (color online).   Left: The marginalized joint likelihood for the present-day value of $Log_{10}B_0$ and the sum of the neutrino masses, $\sum m_\nu$. Center and Right: The marginalized likelihood of $Log_{10}B_0$ for models with variable (a) or fixed (b) neutrino masses. In all three panels different colors correspond to different numerical codes, as shown in the legend and described in Sec. III B. The darker and lighter shades correspond, respectively, to the 68% C.L. and 95% C.L.

disentangle the effects of these two approximations, we have created a quasistatic version of EFTCAMB customized to $f(R)$ theories that implements Eq. (9), which we call QS-$f(R)$; in other words, it assumes the QS regime but it properly models the time dependence of the background terms, so that at the level of the background the modeling is the same as in EFTCAMB and the differences only come from the different treatment of the dynamics of the perturbations. We show a comparison of the results obtained with EFTCAMB, MGCAMB, and QS-$f(R)$ in Fig. 3. It can be noticed that, as expected, results obtained with QS-$f(R)$ lie in between those obtained with EFTCAMB and MGCAMB. Furthermore, it can be seen that in all three panels, MGCAMB and QS-$f(R)$ results are very close to each other, while those obtained with EFTCAMB differ to some extent. Comparing the one-dimensional likelihoods of the center and right panels, we can notice that the difference between EFTCAMB and the other two codes is significantly enhanced when massive neutrinos are added. From these comparisons we can infer that the discrepancy found in Fig. 2 between EFTCAMB and MGCAMB is mostly due to the different modeling of the dynamics of the perturbations; the quasistatic approximation misses out on some important dynamical contributions. However, as can be noticed in the right panel of Fig. 3, in the case with a fixed neutrino mass the QS approximation and the power-law modeling of the background contribute similarly to the difference between EFTCAMB and MGCAMB. We expect the above results to depend to some extent on the data set considered, with the differences potentially being smaller for data sets that have a weaker constraining power on $f(R)$. Nevertheless, given the accuracy and wealth of upcoming measurements it is certainly important to take these discrepancies into account. A more detailed and quantitative analysis of the roles that these two assumptions play is the subject of an ongoing investigation.

IV. A WORKED EXAMPLE II: MASSIVE NEUTRINOS AND PURE EFT MODELS

Another built-in case that can be explored with EFTCAMB is the so-called *pure* EFT mode, in which one directly parametrizes the time dependence of the different functions in the EFT action [15,16]. For simplicity, we will focus on models that only contain the three background operators, i.e., those that affect the dynamics of both the background and the perturbations. The corresponding action is

$$S = \int d^4x \sqrt{-g} \left\{ \frac{m_0^2}{2}[1 + \Omega(\tau)]R + \Lambda(\tau) - a^2 c(\tau)\delta g^{00} \right\}$$
$$+ S_2[g_{\mu\nu}] + S_m[\chi_i, g_{\mu\nu}], \qquad (11)$$

where S_2 contains all EFT operators affecting only the dynamics of the perturbations and S_m is the action for

matter fields, which are minimally coupled to the metric $g_{\mu\nu}$.

As discussed in Ref. [15], we employ a designer approach and (after fixing the desired expansion history) eliminate two of the three EFT functions in favor of the third one, which is typically chosen to be $\Omega(a)$; to fully specify the model we then need to choose a time dependence for the latter [56]. In this paper we investigate degeneracies between massive neutrinos and *pure* EFT models with a linear parametrization of Ω, i.e.,

$$\Omega(a) = \Omega_0^{\rm EFT} a. \qquad (12)$$

This model can be considered as a parametrization of a scalar-tensor theory, where Ω is the coupling function and the kinetic and potential terms are represented, respectively, by the c function and $c - \Lambda$. Following the prescription in Ref. [15], once the background expansion history is chosen the potential and kinetic terms become fixed. While EFTCAMB allows one to choose between several expansion histories, in the following analysis we fix it to match the ΛCDM one.

To test this model we used different combinations of the data set described in Sec. II; the corresponding constraints on $\Omega_0^{\rm EFT}$ and $\sum m_\nu$ are listed in Table II. From there we can see that the bounds on $\Omega_0^{\rm EFT}$ do not sensibly change with respect to the results reported in Ref. [16], where the neutrino masses were set to zero. In that case the bound on $\Omega_0^{\rm EFT}$ was found to be $\Omega_0^{\rm EFT} < 0.061$ (95% C.L.) when considering Planck + WP + BAO + lensing (for details see Table I(a) in Ref. [16]). The only exception is given by the most complete data combination, which slightly improves on the previous bounds. Overall, the constraints on the sum of the neutrino masses are more stringent than in the $f(R)$ case for all the data sets considered, given the lack of degeneracy, as can be noticed in Fig. 4. In particular, the bounds are close to those found in Ref. [5] in the absence of modified gravity. However, when lensing data are added one can notice some weak degeneracy between $\Omega_0^{\rm EFT}$ and $\sum m_\nu$ in the left panel of Fig. 4, which results in this data set favoring a slightly bigger neutrino mass and a smaller value of $\Omega_0^{\rm EFT}$. From the middle and right panels of Fig. 4, we can see that the degeneracy between σ_8 and $\Omega_0^{\rm EFT}$ is also negligible and that the interplay between the neutrino

TABLE II. Constraints on the cosmological parameter of the *pure* linear EFT parametrization with variable neutrino mass, using different combinations of data sets.

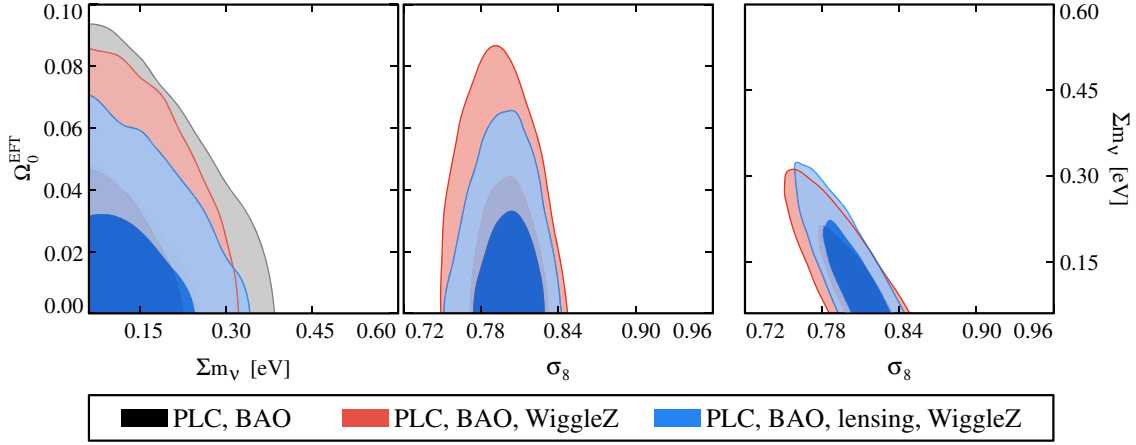| Data sets	Variable m_ν	
	$\Omega_0^{\rm EFT}$ (95% C.L.)	$\sum m_\nu$ (95% C.L.)
PLC + BAO	< 0.06	< 0.30
PLC + BAO + WiggleZ	< 0.06	< 0.25
PLC + BAO + lensing +WiggleZ	< 0.05	< 0.26

FIG. 4 (color online).   The marginalized joint likelihood for the present-day value of Ω_0^{EFT}, the sum of the neutrino masses, $\sum m_\nu$, and the amplitude of the (linear) power spectrum on the scale of $8h^{-1}$ Mpc, σ_8. Different colors correspond to different combinations of cosmological observations, as shown in the legend. The darker and lighter shades correspond, respectively, to the 68% C.L. and 95% C.L. No new significant degeneracies between these parameters are found.

masses and σ_8 is not sensibly altered (with respect to Ref. [5]) by linear EFT models.

In conclusion, our results suggest that no degeneracy with massive neutrinos is present when the linear EFT model on ΛCDM cosmology is considered. One could wonder whether the same model on a different background would result in a different degeneracy. The results in Ref. [16] seem to imply that exploring the same model on wCDM would not alter the bounds very much, since no effects due to a modification of gravity would be appreciable. It would certainly be interesting to explore it on the Chevallier-Polarski-Linder background [57,58]. Another way to find sizable differences from general relativity would be to investigate a more complex temporal evolution of the nonminimally coupling constant $\Omega(a)$ than that in the linear model.

V. CONCLUSIONS

It is well known that the addition of massive neutrinos to the standard cosmological model affects the growth of structures in the Universe. On the other hand, the same imprint on structure formation might also be a characteristic of a class of scalar-tensor theories. This is why the degeneracy between the massive neutrino component and models of modified gravity has been extensively investigated, in particular for $f(R)$ theories.

In this work we used EFTCAMB/EFTCosmoMC to investigate the degeneracy between massive neutrinos and generalized theories of gravity in a ΛCDM background. In particular, we considered designer $f(R)$ models and a simple linear EFT model, effectively consisting of a scalar field whose coupling to gravity changes linearly with the scale factor. In each case, we considered different combinations of the first data release of the Planck satellite,

BAO measurements, and large-scale structure data from Wiggle Z.

In the $f(R)$ case, we found that the combination of Planck and BAO measurements displayed a marked degeneracy between the Compton wavelength of the scalaron and the sum of the neutrino masses. With the addition of large-scale structure data from the WiggleZ experiment we found that this degeneracy is alleviated, resulting in stronger constraints. In particular, the most complete data set that we used results in $\mathrm{Log}_{10}B_0 < -4.1$ at 95% C.L. if the neutrinos are assumed to have a fixed mass equal to $\sum m_\nu = 0.06$ eV, and $\mathrm{Log}_{10}B_0 < -3.8$ and $\sum m_\nu < 0.32$ at 95% C.L. if the neutrino masses are allowed to vary. We compared our results to those obtained by means of MGCAMB, in which $f(R)$ models are typically treated via the parametrization introduced in Ref. [38], which assumes the quasistatic regime and a specific power-law evolution for the characteristic length scale of the model. Overall, there is good agreement between the two codes; however, due to the different modeling there is a slight change in the degeneracy between the $f(R)$ models and massive neutrinos. In particular, this degeneracy changes direction in parameter space, resulting in the fact that EFTCAMB obtains stronger bounds on $\mathrm{Log}_{10}B_0$ but weaker constraints on $\sum m_\nu$. We observed that other degeneracies are also affected by the different physical modeling, so that with EFTCAMB there is less degeneracy between the $f(R)$ models and σ_8.

In the case of the *pure* linear EFT model we found that, in contrast to the $f(R)$ case, there is no appreciable degeneracy between the present-day value of the coupling, Ω_0^{EFT}, and the sum of the neutrino masses for all the data-set combinations that we considered. While a more extensive investigation of different nonminimally coupled pure EFT models is left for future work, we stress that the absence of

degeneracy should be considered unique to the specific parametrization chosen for the coupling (i.e., linear in the scale factor). As a result the constraints on $\Omega_0^{\rm EFT}$ slightly improve with respect to the one previously obtained in Ref. [16], regardless of the presence of massive neutrinos. The combination of the PLC, BAO, lensing, and WiggleZ data then results in $\Omega_0^{\rm EFT} < 0.05$ and $\sum m_\nu < 0.26$ at 95% C.L..

This work was made possible by the release of an updated version of EFTCAMB/EFTCosmoMC, which is publicly available at http://wwwhome.lorentz.leidenuniv.nl/~hu/codes/ and is fully compatible with massive neutrinos for all the built-in modified gravity models. In addition, it includes the complete modeling of the effects of modified gravity on tensor modes and polarization spectra. The designer section of the code has been expanded to include designer minimally coupled quintessence models, and the stability priors have been equipped with several options to control the ones that are not related to mathematical stability. Finally, the updated version includes several new parametrizations for the equation of state of DE that are also fully compatible with designer models.

[1] M. Maltoni, T. Schwetz, M. A. Tortola, and J. W. F. Valle, New J. Phys. **6**, 122 (2004).

[2] G. L. Fogli, E. Lisi, A. Marrone, and A. Palazzo, Prog. Part. Nucl. Phys. **57**, 742 (2006).

[3] J. Lesgourgues and S. Pastor, Phys. Rep. **429**, 307 (2006).

[4] Y. Y. Y. Wong, Annu. Rev. Nucl. Part. Sci. **61**, 69 (2011).

[5] P. A. R. Ade *et al.* (Planck Collaboration), Astron. Astrophys. **571**, A16 (2014).

[6] A. Lewis and A. Challinor, Phys. Rev. D **66**, 023531 (2002).

[7] A. Silvestri and M. Trodden, Rep. Prog. Phys. **72**, 096901 (2009).

[8] B. Jain and J. Khoury, Ann. Phys. (Amsterdam) **325**, 1479 (2010).

[9] B. Jain *et al.*, arXiv:1309.5389.

[10] M. Baldi, F. Villaescusa-Navarro, M. Viel, E. Puchwein, V. Springel, and L. Moscardini, Mon. Not. R. Astron. Soc. **440**, 75 (2014).

[11] J. h. He, Phys. Rev. D **88**, 103523 (2013).

[12] J. Dossett, B. Hu, and D. Parkinson, J. Cosmol. Astropart. Phys. 03 (2014) 046.

[13] A. Hojjati, L. Pogosian, and G. B. Zhao, J. Cosmol. Astropart. Phys. 08 (2011) 005.

[14] H. Motohashi, A. A. Starobinsky, and J. Yokoyama, Phys. Rev. Lett. **110**, 121302 (2013).

[15] B. Hu, M. Raveri, N. Frusciante, and A. Silvestri, Phys. Rev. D **89**, 103530 (2014).

[16] M. Raveri, B. Hu, N. Frusciante, and A. Silvestri, Phys. Rev. D **90**, 043513 (2014).

[17] http://camb.info.

[18] A. Lewis, A. Challinor, and A. Lasenby, Astrophys. J. **538**, 473 (2000).

[19] A. Lewis and S. Bridle, Phys. Rev. D **66**, 103511 (2002).

[20] G. Gubitosi, F. Piazza, and F. Vernizzi, J. Cosmol. Astropart. Phys. 02 (2013) 032.

[21] J. K. Bloomfield, É. É. Flanagan, M. Park, and S. Watson, J. Cosmol. Astropart. Phys. 08 (2013) 010.

[22] F. Piazza and F. Vernizzi, Classical Quantum Gravity **30**, 214007 (2013).

[23] H. K. Jassal, J. S. Bagla, and T. Padmanabhan, Mon. Not. R. Astron. Soc. **356**, L11 (2005).

[24] H. K. Jassal, J. S. Bagla, and T. Padmanabhan, Mon. Not. R. Astron. Soc. **405**, 2639 (2010).

[25] Y. Hu, M. Li, X.-D. Li, and Z. Zhang, Sci. China Phys. Mech. Astron. **57**, 1607 (2014).

[26] B. Hu, M. Raveri, N. Frusciante, and A. Silvestri, arXiv:1405.3590.

[27] P. A. R. Ade *et al.* (Planck Collaboration), Astron. Astrophys. **571**, A15 (2014).

[28] G. Hinshaw *et al.* (WMAP Collaboration), Astrophys. J. Suppl. Ser. **208**, 19 (2013).

[29] P. A. R. Ade *et al.* (Planck Collaboration), Astron. Astrophys. **571**, A17 (2014).

[30] F. Beutler, C. Blake, M. Colless, D. H. Jones, L. Staveley-Smith, L. Campbell, Q. Parker, W. Saunders, and F. Watson, Mon. Not. R. Astron. Soc. **416**, 3017 (2011).

[31] W. J. Percival *et al.* (SDSS Collaboration), Mon. Not. R. Astron. Soc. **401**, 2148 (2010).

[32] N. Padmanabhan, X. Xu, D. J. Eisenstein, R. Scalzo, A. J. Cuesta, K. T. Mehta, and E. Kazin, Mon. Not. R. Astron. Soc. **427**, 2132 (2012).

[33] L. Anderson *et al.*, Mon. Not. R. Astron. Soc. **427**, 3435 (2012).

[34] http://smp.uq.edu.au/wigglez-data.

[35] M. J. Drinkwater *et al.*, Mon. Not. R. Astron. Soc. **401**, 1429 (2010).

[36] D. Parkinson *et al.*, Phys. Rev. D **86**, 103518 (2012).

[37] C. Blake *et al.*, Mon. Not. R. Astron. Soc. **406**, 803 (2010).

[38] E. Bertschinger and P. Zukin, Phys. Rev. D **78**, 024015 (2008).

[39] G. B. Zhao, L. Pogosian, A. Silvestri, and J. Zylberberg, Phys. Rev. D **79**, 083513 (2009).

[40] T. P. Sotiriou and V. Faraoni, Rev. Mod. Phys. **82**, 451 (2010).

[41] A. De Felice and S. Tsujikawa, Living Rev. Relativity **13**, 3 (2010).

[42] L. Lombriser, Ann. Phys. (Amsterdam) **526**, 259 (2014).

[43] A. A. Starobinsky, JETP Lett. **86**, 157 (2007).

[44] Y.-S. Song, W. Hu, and I. Sawicki, Phys. Rev. D **75**, 044004 (2007).

[45] R. Bean, D. Bernat, L. Pogosian, A. Silvestri, and M. Trodden, Phys. Rev. D **75**, 064020 (2007).

[46] L. Pogosian and A. Silvestri, Phys. Rev. D **77**, 023503 (2008); Phys. Rev. D **81**, 049901(E) (2010).

[47] E. Komatsu *et al.* (WMAP Collaboration), Astrophys. J. Suppl. Ser. **192**, 18 (2011).

[48] C. Howlett, A. Lewis, A. Hall, and A. Challinor, J. Cosmol. Astropart. Phys. 04 (2012) 027.

[49] G. Mangano, G. Miele, S. Pastor, and M. Peloso, Phys. Lett. B **534**, 8 (2002).

[50] G. Mangano, G. Miele, S. Pastor, T. Pinto, O. Pisanti, and P. D. Serpico, Nucl. Phys. **B729**, 221 (2005).

[51] T. Giannantonio, M. Martinelli, A. Silvestri, and A. Melchiorri, J. Cosmol. Astropart. Phys. 04 (2010) 030.

[52] R. Bean and M. Tangmatitham, Phys. Rev. D **81**, 083534 (2010).

[53] A. Hojjati, L. Pogosian, A. Silvestri, and S. Talbot, Phys. Rev. D **86**, 123503 (2012).

[54] L. Lombriser, A. Slosar, U. Seljak, and W. Hu, Phys. Rev. D **85**, 124038 (2012).

[55] B. Hu, M. Liguori, N. Bartolo, and S. Matarrese, Phys. Rev. D **88**, 123514 (2013).

[56] N. Frusciante, M. Raveri, and A. Silvestri, J. Cosmol. Astropart. Phys. 02 (2014) 026.

[57] M. Chevallier and D. Polarski, Int. J. Mod. Phys. D **10**, 213 (2001).

[58] E. V. Linder, Phys. Rev. Lett. **90**, 091301 (2003).